PAPER

Check for updates

An injectable, self-healing, polysaccharide-based antioxidative hydrogel for wound healing†

Melissa Johnson,[a,b] Rijian Song,[a,b,c,d] Yinghao Li,[a] Cameron Milne,[a,b] Zishan Li,[a] Jing Lyu, [a] Sigen A[a,b] and Wenxin Wang *[a,c,d]

Advanced treatment of chronic wounds is critical to maintaining the physical and mental health of patients and improving their quality of life. Consequently, wound dressings with multifunctional properties are highly desired to achieve high wound closure effectiveness in chronic wound healing clinical applications. Therefore, an antioxidative dynamic hydrogel composed of aldehyde functionalised hyaluronic acid (HA-CHO) and disulfide functionalised chondroitin sulfate (CS-DTP) was designed. A disulfide moiety was utilised to functionalise chondroitin sulfate to introduce antioxidative functionality to the hydrogel scaffold. The dynamic covalent chemistry of the hydrazone network, which forms between the aldehyde and hydrazide functional groups, provides the hydrogel system with the desired properties of *in situ* rapid gelation and self-healing. The functional group content, rheology, self-healing, responsive degradation rate, ROS scavenging activity and cell biocompatibility of the hydrogels were characterised. Overall, this work demonstrates the facile preparation of a new dynamic hydrogel system, presenting a promising solution for wound care therapy as an antioxidative wound dressing.

1. Introduction

Wound healing is a complex and dynamic process with four overlapping phases: hemostasis, inflammation, proliferation, and remodelling.[1] Due to the complexity of the wound healing process, any disruption can lead to chronic wounds. Chronic wounds are characterised by persistent inflammation and the production of excessive reactive oxygen species (ROS) (*e.g.* superoxide anion ($O_2^{\cdot-}$), hydroxyl radical ($OH^{\cdot}$), and hydrogen peroxide (H_2O_2)), resulting in oxidative stress.[2] Given that skin tissues are susceptible to oxidative stress, excessive ROS production has been shown to impair wound healing processes by cellular damage, resulting in clinical conditions such as tissue

hypoxia[3] and hyperglycemia.[4] Therefore, effective wound care treatment strategies for the elimination of excessive ROS must be developed.

Antioxidant materials can stabilise, deactivate, or scavenge free radicals and restore the normal physiological level of ROS.[5] Hence, antioxidant-based therapies have shown promising results in promoting skin wound healing, though clinical studies still remain limited.[6] To date, different types of antioxidative wound dressings have been explored, such as films,[7] membranes,[8] fibres,[9] sponges,[10] and hydrogels.[11,12] Hydrogel wound dressings with antioxidant functions, emerged as a competitive candidate to accelerate chronic wound healing. Hydrogels, especially, have a high water content that can create a moist wound healing environment due to their unique three-dimensional (3D) networks of hydrophilic polymers.[13] Dynamic covalent cross-linking hydrogels have recently emerged as highly promising materials for clinical hydrogel wound dressings.[14] These hydrogels incorporate dynamic covalent bonds that can reversibly break and reform in response to specific stimuli, granting them exceptional properties such as self-healing and injectability.[15]

In recent years, a range of ROS (*e.g.* H_2O_2) responsive moieties incorporated into hydrogel scaffolds have been studied, including disulfide,[16] boronic ester/acids,[17] thioether,[18] diselenide,[19,20] and thioketal groups[21] *etc.* The H_2O_2 responsive moieties are typically incorporated into hydrogels *via* two approaches: (1) as pendant or terminal groups in the poly-

[a]Charles Institute of Dermatology, School of Medicine, University College Dublin, D04 V1W8 Dublin, Ireland. E-mail: wenxin.wang@ucd.ie

[b]Blafar Ltd, Pioneer Life Sciences Cherrywood, Cherrywood Business Park, Loughlinstown, D18 T3Y1 Dublin, Ireland

[c]Joint Research Center for Occupational Medicine and Health of IHM, Anhui University of Science and Technology, Huainan, China

[d]Institute of Precision Medicine (AUST-IPM), Anhui University of Science and Technology, Huainan, China

†Electronic supplementary information (ESI) available: Supplementary experiment section, Fig. S1: Strain-amplitude sweep test of CS-ADH/HA-CHO; Fig. S2: Oscillation strain–strain test of CS-ADH/HA-CHO; Fig. S3: Mechanical property test of CS-ADH/HA-CHO; Fig. S4: Quantitative cell viability evaluation by alamarBlue assay; Fig. S5: Live/dead staining images; and supplementary references. See DOI: https://doi.org/10.1039/d4lp00337c

meric chains which can then be involved in the crosslinking reactions to fabricate the 3D hydrogel scaffolds, or (2) as difunctional crosslinkers (*e.g.* cystamine dihydrochloride).[22,23]

R. Yang *et al.*, developed a multifunctional dynamic antioxidative hydrogel for promoting skin wound healing.[24] Polylisine-*graft*-cysteine and oxidised dextran were dynamically crosslinked by Schiff-base reaction. However, the gelation time of the dynamic hydrogels ranged from 60–300 s. A longer gelation time may cause precursor solution to diffuse from the target sites, compromising the therapeutic effect and inducing wound infection. Therefore, we hypothesise that by increasing functional group content within a hydrogel network the hydrogel gelation time can be decreased for rapid wound coverage.

In our previous work, Q. Xu *et al.*, reported a synthetic method for the fabrication of a novel class of ROS-cleavable hyperbranched poly(β-hydrazide esters).[25] These synthetic polymers were crosslinked with thiolated hyaluronic acid *via* thiol–ene click chemistry for the development of injectable antioxidative hydrogels. The hydrogels demonstrated remarkable antioxidative efficiency and excellent bio-compatibility; nevertheless, we hypothesise that to further promote wound healing an effective antioxidative hydrogel can be achieved by utilising only naturally-derived functionalised biopolymers (*e.g.* hyaluronic acid and chondroitin sulfate), as naturally-derived polymer networks will impart inherent biodegradability and biocompatibility into the scaffold.

Therefore, in this study, a polysaccharide-based dynamic covalent hydrazone crosslinked hydrogel was developed to meet the requirements for an ideal wound dressing. This hydrogel (1) forms *in situ* with fast gelation, (2) exhibits self-healing properties, (3) provides antioxidative effects, (4) undergoes responsive degradation (5) is biocompatible, and (6) can incorporate active substances that can promote wound healing, such as stem cells, drugs, growth factors, and exosomes. The hydrogels were prepared by mixing aldehyde-functionalised hyaluronic acid solution and disulfide-functionalised chondroitin sulfate solution (CS-DTP) (Scheme 1).

To provide antioxidative capabilities to the hydrogel, a hydrazide monomer with disulfide containing moiety (3,3′-dithiobis(propanoic dihydrazide) (DTP)) was utilised to disulfide functionalise chondroitin sulfate. This approach was inspired by studies such as Y. Yang *et al.*, where cystamine was grafted onto hyaluronic acid through amidation, creating Schiff base reaction sites for crosslinking and imparting antioxidant properties.[26] However, by utilising the dynamic covalent chemistry of hydrazone formation in our hydrogel system rather than Schiff base, the hydrogel mechanical characteristics may be improved, as hydrazone crosslinks exhibit better intrinsic stability than Schiff base crosslinks.[27]

The functional group content, rheology, degradation, ROS scavenging activity and cell biocompatibility of the hydrogels were characterised and compared to a control (hydrazide functionalised chondroitin sulfate ((CS-ADH) without disulfide moiety)). Significantly, the CS-DTP/HA-CHO exhibited a remarkable increase in cell viability of the encapsulated cells when exposed to ROS, in contrast to the hydrogel without disulfide moiety (CS-ADH). The properties of fast gelation, self-healing, injectability, responsive degradation, ROS scavenging ability, and excellent bio-compatibility has shown that this hydrogel (CS-DTP/HA-CHO) possesses a potential application in wound repair, particularly for wound care treatment as an antioxidative wound dressing.

2. Experimental

2.1 Materials

Chondroitin sulfate C sodium salt (Biosynth). Hyaluronic acid (220 kDa, food grade, Stanford Chemical Ltd). Adipic dihydrazide, sodium (*meta*) periodate (99.5%), ethylene glycol (99.8%), 1-ethyl-3-[3-(dimethylamino)propyl]carbodiimide (EDCI), hydrochloric acid (34%), sodium hydroxide (≥98%), *t*-butyl carbazate (98%), 2,4,6-trinitrobenzenesulfonic acid solution (TNBS, 5% w/v in H_2O), sodium tetraborate decahydrate (≥99.5%), trichloroacetic acid (98%), hydrogen peroxide (H_2O_2, 50% wt% in H_2O), 2,2-diphenyl-1-picrylhydrazyl (DPPH), and phosphate-buffered saline (PBS), were purchased from Sigma-Aldrich and used without further purification. Dialysis tubing (cut off M_w 8 kDa) was purchased from Spectrum Lab. Human keratinocyte cells (HaCaT) and normal human dermal fibroblasts (NHDFs) were purchased from ATCC and rat adipose derived stem cells (rADSCs) were purchased from Cyagen. Dulbecco's modified Eagle's medium (DMEM), fetal bovine serum (FBS), and penicillin/streptomycin were purchased from Invitrogen. The AlamarBlue reagent, live/dead viability cytotoxicity kit, and HyStem® cell culture scaffold kit were obtained from Sigma-Aldrich.

2.2 Instruments

Rheological assessments were performed using a TA HR-2 rheometer fitted with an 8 mm steel parallel-plate geometry. Absorbance data were collected with a micro-plate reader (molecular devices SpectraMax M3). To detect cell staining, a Leica microscope (DM2500 fluorescence) was utilised.
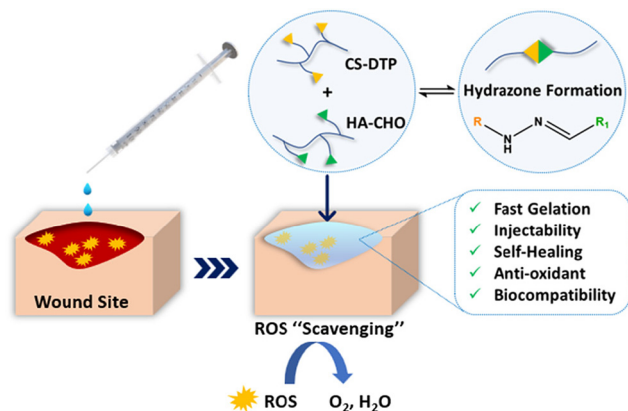
Scheme 1 Schematic illustration of the fabrication and application of the CS-DTP/HA-CHO hydrogel. (R = CS-DTP, R_1 = HA-CHO).

© 2025 The Author(s). Published by the Royal Society of Chemistry

RSC Appl. Polym., 2025, **3**, 238–246 | **239**

2.3 Methods

2.3.1 Synthesis of disulfide functionalised chondroitin sulfate (CS-DTP) and hydrazide functionalised (CS-ADH).

Two types of functionalised chondroitin sulfate were synthesised with two types of hydrazide monomers, 3,3′- dithiobis(propanoic dihydrazide) (DTP) and adipic dihydrazide (ADH). Chondroitin sulfate C (CS) (1 g) was dissolved in deionised H_2O (100 mL) and then DTP or ADH (20 mmol) was added while stirring the solution. The pH of the reaction mixture was adjusted to 4.75 by adding 1.0 M HCl. Next, EDCI (2 mmol) was added to the mixture solution. The pH of the reaction mixture was kept at 4.75 for 2 hours by the addition of 1.0 M HCl aliquots. The reaction was then stopped by the addition of 1.0 M NaOH to increase the pH to 7.0. The solution mixture was transferred to dialysis tubing (cut off M_w 8 kDa) and dialysed against deionised H_2O for 4 days. The dialysed solution was lyophilised to obtain a white solid foam. The products were named CS-DTP and CS-ADH.

2.3.2 Synthesis of aldehyde-functionalised hyaluronic acid (HA-CHO).

HA-CHO was synthesised following a previously published procedure with minor modifications.[32] Hyaluronic acid (HA) ((220 kDa), 2 g) was dissolved in deionised H_2O (200 mL), and then sodium periodate (1 equiv.) was added slowly. The reaction mixture was stirred overnight at RT in the dark. Afterward, ethylene glycol (1 mL) was added to react with the excess periodate, and the solution was stirred for an additional hour. For purification, the reaction mixture was placed in dialysis tubing (cut off M_w 8 kDa) and dialysed against deionised H_2O for 4 days. The dialysed solution was lyophilised to obtain a white solid foam, which was stored under argon atmosphere.

2.3.3 Characterisation of HA-CHO, CS-DTP and CS-ADH by 2,4,6-trinitrobenzene sulfonic acid (TNBS) assay.

30 μL (0.6%) HA-CHO and 30 μL (30 mM) t-butyl carbazate (t-BC) in aqueous trichloroacetic acid (1%) were mixed and allowed to react at room temperature. After 24 h, 0.6 mL TNBS solution (6 mmol, 0.1 M borate buffer, pH 8) was added to the mixture to react with the excess t-BC. The reaction solution was then allowed to react for 1 h at room temperature. Subsequently, 200 μL of the mixture was diluted with 400 μL of 0.5 N HCl and allowed to react for 30 min. Finally, 150 μL of the resulting mixture was transferred to a 96-well plate, and the absorbance was measured at 340 nm using a spectro-photometer microplate reader. A standard calibration curve derived from aqueous t-BC solutions (5–30 mM) was used to quantify the unreacted t-BC and calculate aldehyde content. All experiments were completed in triplicate.

30 μL (0.6%) CS-DTP and CS-ADH was added to 0.6 mL of a TNBS solution (6 mmol, 0.1 M borate buffer, pH 8). The CS-DTP and CS-ADH reaction solutions were allowed to react for 1 h at room temperature. The solutions were diluted and the absorbance was measured as abovementioned. A standard calibration curve based on aqueous t-BC solutions (5–30 mM) was used to determine the amine content. All experiments were conducted in triplicate.

2.3.4 Hydrogel fabrication of CS-DTP/HA-CHO and CS-ADH/HA-CHO.

The HA-CHO solutions were prepared by dissolving the synthesised HA-CHO in PBS (3% w/v). CS-DTP and CS-ADH solutions were prepared by dissolving the synthesised CS-DTP and CS-ADH in PBS (4% w/v). The hydrogel was prepared by mixing equal volumes of CS-DTP or CS-ADH solution with the HA-CHO solution at RT (1 : 1 volume ratio).

2.3.5 Hydrogel rheological assessments.

Mechanical properties of the prepared hydrogels were measured using a TA rheometer (HR-2) with an 8 mm parallel plate. The premixed solution was applied to the plate for time sweep tests, conducted immediately at 25 °C with a frequency of 1.0 Hz and 1% strain. A strain sweep test from 1% to 100% strain at 1.0 Hz was used to assess the linear viscoelastic range. Self-healing properties were evaluated by applying continuous oscillatory strain cycles between 1% and 100% at 1.0 Hz, with each step lasting 60 seconds. A 1000 μm gap was maintained for all tests, which were performed in triplicate at 25 °C.

2.3.6 Visual hydrogel self-healing test.

The spontaneous self-healing behaviour was visually determined. Round hydrogel disks (~2.5 cm diameter) of CS-DTP/HA-CHO were stained in colour to aid visual examination. The hydrogel disks were cut into quarters, and placed in contact with different colours. Photos were taken to monitor the self-healing process.

2.3.7 Responsive hydrogel swelling and degradation study.

Swelling and degradation studies were conducted on CS-DTP/HA-CHO and CS-ADH/HA-CHO hydrogels in medium solutions (1× PBS buffer; 0.1 mM, 0.5 mM, 1 mM H_2O_2 solution in 1× PBS buffer) under 37 °C. To assess the swelling and degradation profile, 2 mL of the medium solution was added to glass vials containing the hydrogels, fully immersing them. The vials were then placed in a shaker set to 37 °C and 150 rpm. At each designated time point, the hydrogels were removed, gently blotted with filter paper to eliminate surface water, and weighed (W_t). Each sample was tested in triplicate. The swelling profile and degradation rate were calculated using the following equation:

$$\text{Percentage of hydrogel mass } (\%) = W_t/W_0 \times 100\%$$

where W_t is the weight at the scheduled time point, and W_0 is the initial weight of the hydrogel.

2.3.8 DPPH radical scavenging activity.

Briefly, a series of DPPH solutions were prepared by dissolving DPPH in methanol, with the final concentrations of 0.1, 0.3, 0.5, and 1 mM. CS-DTP and CS-ADH hydrogels (100 μL) were prepared and immersed in 1 mL DPPH solution. PBS (100 μL) was added to the DPPH solutions as the blank control group. The reaction mixture was continuously shaken in the dark at 37 °C for 30 min. The absorbance of the solution was then measured at 517 nm using a spectrophotometer microplate reader. Each sample was tested in triplicate. The DPPH radical scavenging activity was calculated using the following equation:

$$\text{DPPH radical scavenging activity } (\%)$$
$$= (A_{blank} - A_{sample})/A_{blank} \times 100\%$$

where A_{blank} is the absorbance of the DPPH solution without the sample (DPPH + methanol), and A_{sample} is the absorbance of the sample solution (DPPH + methanol + hydrogel).

2.3.9 Cytotoxicity test of CS-DTP, CS-ADH and HA-CHO polymer solutions. The cytotoxicity assessment of CS-DTP, CS-ADH and HA-CHO polymer solutions was tested using HaCaT cells by alamarBlue assay. All solutions for cell viability tests were prepared in PBS buffer and sterilised by filtration through a 0.22 μm pore-size filter. The positive control (100% viability) was defined as cells without treatment. HaCaTs were seeded in a 96-well plate at the density of 1×10^4 cells per well and cultured in full cell media (DMEM with 10% FBS and 1% penicillin/streptomycin) under standard cell culture conditions (37 °C, 5% CO_2). Following overnight culture, the cell media was changed to a series of CS-DTP or CS-ADH or HA-CHO solutions (from 100 to 1000 μg mL^{-1} in full cell media, $n = 3$). The cell viability was tested at 24 h and 72 h after co-culture using alamarBlue. After 4 h of incubation, the absorbance was measured at 570 nm with a microplate reader. To assess cell viability, live/dead staining (calcein/ethidium) was used. At 24 and 72 hours, the culture medium was removed and replaced with the live/dead stain. After a 30 min incubation at 25 °C, the stain was washed off the well plates with PBS. The images were captured using a fluorescence microscope.

2.3.10 Hydrogel ROS protection against H_2O_2 induced damage of rADSCs and NHDFs. Rat adipose-derived stem cells (rADSCs) and normal human dermal fibroblasts (NHDFs) were cultured and the cells were collected by centrifugation before being encapsulated into the hydrogel precursor and resuspended in the PBS buffer, respectively. CS-DTP (4% w/v), CS-ADH (4% w/v) and HA-CHO (3% w/v) were fully dissolved in fresh medium and then filtered by 0.22 μm filter. The HA-CHO solution, CS-DTP or CS-ADH and cell suspension (rADSCs or NHDFs) were mixed to obtain a final cell density of 2.0×10^5. 2D cultured cells were used as the control. After 30 min, the cell-encapsulated hydrogels were placed in a 24-well plate and incubated at 37 °C with 600 μL of full cell media (DMEM containing 10% FBS and 1% penicillin/streptomycin) per well ($n = 3$) for 24 hours. The culture media was then replaced with DMEM supplemented with 1 mM H_2O_2, 10% FBS, and 1% penicillin/streptomycin. After 24 h co-culture, alamarBlue assay and live/dead staining were conducted as abovementioned to determine the ROS protections of the hydrogels.

2.3.11 Statistical analysis. The obtained values ($n > 3$) are expressed as mean ± standard deviation (SD). ROS protection hydrogel analysis, statistical differences between two groups were deter-mined using the student's unpaired t test. A value of *$p < 0.05$, **$p < 0.01$, or ***$p < 0.001$ was considered statistically significant.

3. Results and discussion

3.1 Synthesis and characterisation of CS-DTP, CS-ADH, and HA-CHO

Aldehyde functionalised hyaluronic acid (HA-CHO) was synthesised through the oxidation reaction of hyaluronic acid (HA) (Scheme 2a), using sodium periodate (NaIO$_4$) which oxidises the adjacent hydroxyl groups at carbon 2 and 3 of the

D-glucuronic acid unit to form a periodate ester.[28] A cyclic mechanism then cleaves the C–C sigma bond, resulting in the formation of two aldehyde groups. After dialysis and freeze-drying, the purified product was obtained as white foam. The aldehyde content (mmol g^{-1}) of HA-CHO was measured by TNBS assay. The aldehyde functional group content of the resulting HA-CHO was 0.94 mmol g^{-1}.

Disulfide functionalised chondroitin sulfate (CS-DTP) was obtained using EDCI chemistry, whereby the hydrazide groups were coupled to the carboxyl groups on the disaccharide repeating units. Chondroitin sulfate (CS) was mixed with the disulfide bond containing hydrazide monomer (3,3′-dithiobis (propanoic hydrazide (DTP))) (Scheme 2b). The pH of the reaction mixture was maintained at 4.75 for two hours by adding 1M HCl. The reaction was then stopped by raising the solution's pH to 7.0 with 1M NaOH. For the control comparison, the commonly utilised hydrazide monomer adipic dihydrazide (ADH) (without disulfide bond) was selected to obtain CS-ADH following the same synthesis approach (Scheme 2c). The purified products were obtained as white foam after dialysis and free-drying, and the amine content (mmol g^{-1}) was quantified by TNBS assay. The amine content of the resulting CS-DTP and CS-ADH was 0.71 mmol g^{-1} and 0.69 mmol g^{-1}, respectively.

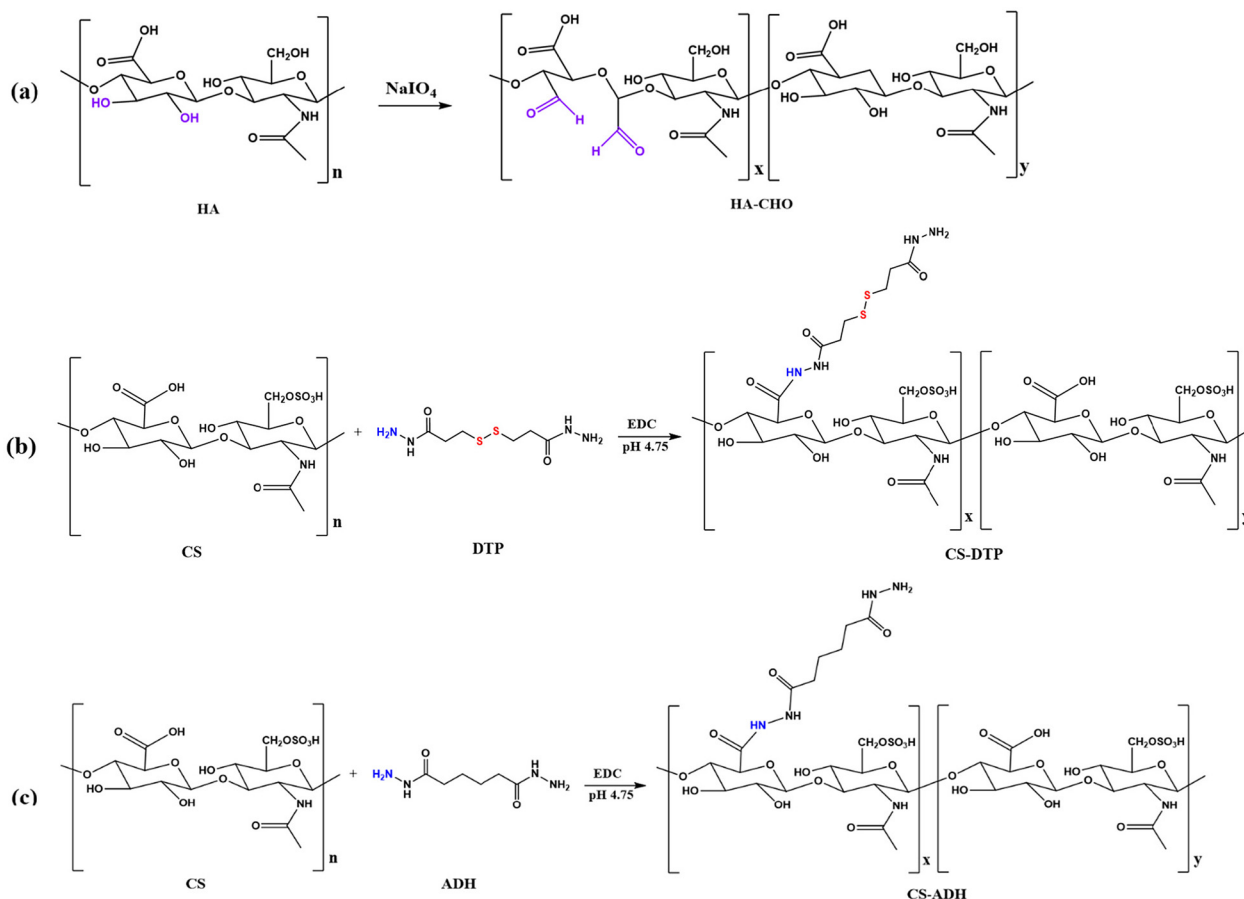## 3.2 Fabrication of CS-DTP/HA-CHO and CS-ADH/HA-CHO Hydrogels

CS-DTP/HA-CHO and CS-ADH/HA-CHO hydrogels were fabricated from CS-DTP or CS-ADH concentration (4% w/v) and HA-CHO concentration (3% w/v) at 1 : 1 volume ratio. As one aldehyde group can react with one hydrazide group, the concentrations and volume ratio of the hydrogel system were selected to achieve the maximum cross-linking ratio of the aldehyde and hydrazide groups. As a result, the crosslinking net-work reaction occurs *via* hydrazone formation at approximately 1 : 1 (–CHO/–NH$_2$) molar ratio (Scheme 1).

Both CS-DTP (4% w/v), CS-ADH (4% w/v), and HA-CHO (3% w/v) PBS solutions were flowable liquids, with a pre-gel solution mixture pH of ~6.7. The gelation time was monitored by using a magnetic stirrer bar to mix the HA-CHO solution in a glass vial. Upon adding CS-DTP or CS-ADH, the viscosity of the solution increased rapidly, causing the magnetic stirrer bar to stop stirring. The gelation time for CS-DTP/HA-CHO and CS-ADH/HA-CHO was 9 s (±2 s, $n = 3$). The rapid gelation time observed allows for the quick application of the multifunctional hydrogel in clinical settings, making it suitable for biomedical applications such as wound healing.

3.3 Rheological assessment of CS-DTP/HA-CHO and CS-ADH/HA-CHO hydrogels

To investigate the gelation behaviour, the time-sweep rheological test of the CS-DTP/HA-CHO and CS-ADH/HA-CHO hydrogels was conducted. As depicted in Fig. 1a, the solution mixtures transitioned to a solid-like state, with the storage modulus (G') surpassing the loss modulus (G''). This rapid sol–gel transition was observed for both hydrogels due to the high

© 2025 The Author(s). Published by the Royal Society of Chemistry

RSC Appl. Polym., 2025, **3**, 238–246 | **241**

Scheme 2 (a) Synthesis of aldehyde functionalised hyaluronic acid (HA-CHO); (b) synthesis of disulfide functionalised chondroitin sulfate (CS-DTP), (monomer: 3,3′-dithiobis(propanoic dihydrazide (DTP))); (c) synthesis of hydrazide functionalised chondroitin sulfate (CS-ADH), (monomer: adipic dihydrazide (ADH)).

functional group content of the CS-DTP, CS-ADH and HA-CHO materials. Subsequently, the hydrogels formed a stable network structure as the G' increased and reached a stable plateau within 900 s. Overall, the G' of CS-DTP/HA-CHO is similar to the G' of CS-ADH/HA-CHO at 24 h, as shown in Fig. 1b, due to the comparable hydrazide functional group content of both CS-DTP and CS-ADH.
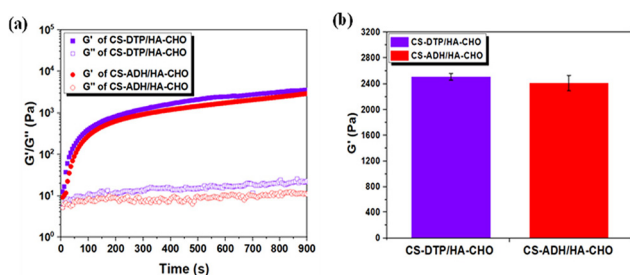

Fig. 1 (a) Time-sweep tests of the CS-DTP/HA-CHO and CS-ADH/HA-CHO hydrogels (25 °C, 1% strain, and 1 Hz); (b) storage modulus (G') of CS-DTP/HA-CHO and CS-ADH/HA-CHO hydrogels at 24 hours (25 °C, 1% strain, and 1 Hz).

The strain-sweep test (Fig. S1†), conducted 2 hours after hydrogel formation indicates the viscoelastic region of the hydrogel samples. The test was conducted by in-creasing oscillatory strain at a constant frequency. The intersection of G' and G'' at 16% and 25% occurs for hydrogel samples CS-DTP/HA-CHO and CS-ADH/HA-CHO, respectively. Since CS-DTP/HA-CHO has a slightly higher crosslinking density (Fig. 1a and b), it undergoes less strain before the G'/G'' crossover point because the hydrogel network is slightly stiffer compared to CS-ADH/HA-CHO, resulting in greater deformation than lower crosslinked networks. Subsequently, the rheological results show that the disulfide bond in CS-DTP/HA-CHO has no significant effect on the mechanical properties of the crosslinked network when compared to CS-ADH/HA-CHO. As a result, in the following studies, CS-ADH/HA-CHO can be utilised as a comparable control.

3.4 Self-healing property of the CS-DTP/HA-CHO and CS-ADH/HA-CHO hydrogels

The rapid self-healing ability of the hydrogels was assessed using an oscillation step-strain test to evaluate the recovery of rheological properties after damaging the hydrogel network with a higher strain (Fig. 2a and Fig. S2†). The test started with
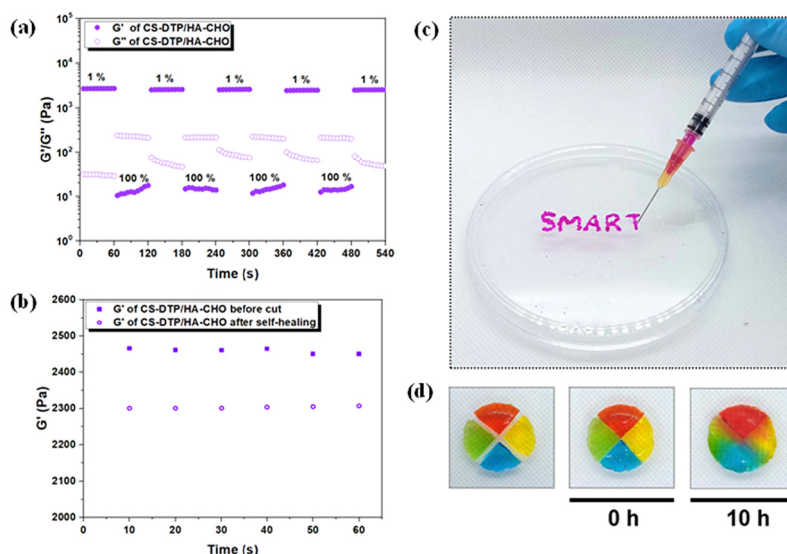
Fig. 2 (a) Oscillation step-strain test of applied strain from 1% to 100% for 540 seconds for CS-DTP/HA-CHO (25 °C, 1 Hz); (b) mechanical property test, before cut and after self-healing of CS-DTP/HA-CHO; (c) CS-DTP/HA-CHO hydrogel was injected through a 28 gauge needle. The hydrogel was stained for observation. (d) Photographs of the self-healing process of CS-DTP/HA-CHO at room temperature.

1% strain for 60 s, followed by the application of a higher strain (100%) application for 60 s. As increased strain is applied, the G' decreased and became lower than G'' for both hydrogels. The G' recovered rapidly once the strain was released, and this recovery process remained consistent over the four step-strain cycles, demonstrating the excellent self-healing capability of the hydrogels due to their dynamic cross-linking network. To further assess the mechanical properties before and after self-healing, the G' was monitored after the hydrogel was cut in half and rejoined (Fig. 2b and Fig. S3†). The minimal difference in G' before and after the cut indicated that the hydrogel network was nearly fully restored. In addition, the CS-DTP/HA-CHO hydrogel could easily be injected through a 28-gauge needle (Fig. 2c). The hydrogel's injectability ensures easy application and conformation to complex wound geometries, a distinct advantage over traditional rigid dressings.

To visually demonstrate the self-healing ability of the dynamic hydrogel, CS-DTP/HA-CHO disks were fabricated and colour stained (Fig. 2d). The coloured hydrogel disks were cut into four quarters, and placed in contact with different colours and left at room temperature. After 10 hours, the four hydrogels had healed spontaneously and merged into a bulk hydrogel without external intervention. The hydrogel contact surfaces were clearly fused as indicated by the colour diffusion, which demonstrated the excellent self-healing ability within the dynamic hydrogel system.

3.5 Responsive hydrogel swelling and degradation study

The *in vitro* swelling properties and degradation behaviour of CS-DTP/HA-CHO and CS-ADH/HA-CHO hydrogels were evaluated by measuring the percentage of hydrogel mass (%) over time under physiological conditions (Fig. 3a). CS-DTP/HA-CHO and CS-ADH/HA-CHO had a degradation time of

~70 h. The degradation profile of both hydrogels was comparable as they have a similar crosslinking density. Both hydrogel systems demonstrate good swelling properties, suggesting that the hydrogels can protect wounds against the accumulation of excess exudate, indicating a potential ability to absorb wound exudate (Fig. 3b).

It is particularly advantageous for wound dressing hydrogel functions to respond to H_2O_2 overexpression in the dynamic wound microenvironment. Therefore, in the H_2O_2 responsive study of CS-DTP/HA-CHO, the hydrogels were immersed in H_2O_2 (0.1, 0.5, and 1 mM), and the CS-ADH/HA-CHO hydrogel was used as the control comparison. According to the responsive swelling and degradation profile shown in Fig. 3c, H_2O_2 (0.5 mM) can accelerate the degradation process of CS-DTP/HA-CHO approximately 25 times faster than CS-ADH/HA-CHO. In comparison the CS-ADH/HA-CHO hydrogel showed similar degradation rate in both PBS and H_2O_2 (0.5 mM). This demonstrates that the disulfide containing moiety in CS-DTP in the CS-DTP/HA-CHO hydrogel can provide a significant difference in the responsive degradation property. As expected, the CS-DTP/HA-CHO hydrogel degraded faster as the H_2O_2 concentration increased (Fig. 3d), and the H_2O_2 responsive degradation time was manipulated from 75 h to 1 h. These results demonstrate that the CS-DTP/HA-CHO hydrogel has an excellent ability to respond to the ROS wound microenvironment.

3.6 DPPH radical scavenging activity

Antioxidant hydrogels can regulate the excessive production of ROS, and reduce their adverse effects to accelerate tissue regeneration.[29] The antioxidation properties of the hydrogels were evaluated by scavenging stable 2,2-diphenyl-1-picrylhydrazyl (DPPH) free radicals. At DPPH concentrations 0.1, 0.3, 0.5, and 1 mM, the CS-DTP/HA-CHO hydrogel showed efficient DPPH scavenging

Fig. 3 Swelling and degradation profiles. (a) CS-DTP/HA-CHO and CS-ADH/HA-CHO from 0 h to 72 h (PBS, 37 °C); (b) CS-DTP/HA-CHO and CS-ADH/HA-CHO from 0 h to 3 h (PBS, 37 °C); (c) CS-DTP/HA-CHO and CS-ADH/HA-CHO (0.5 mM H_2O_2, 37 °C); (d) CS-DTP/HA-CHO (PBS, 0.1, 0.5, and 1 mM H_2O_2, 37 °C).

ability of 91%, 88%, 75%, and 66%, respectively (Fig. 4a). The ability of CS-DTP/HA-CHO hydrogels to scavenge DPPH free radicals is attributed to the electron transfer donated from the disulfide group in CS-DTP to the free radicals. Compared to the CS-DTP/HA-CHO hydrogel, CS-ADH/HA-CHO demonstrated less scavenging of DPPH, although moderate antioxidant capability was displayed due to the hydrazide functional groups that is consistent with previous studies.[30–32]

Fig. 4b depicts the DPPH radical solution absorption curves of CS-DTP/HA-CHO hydrogel solution compared to the solution without hydrogel sample. It shows that DPPH free radicals have strong absorption at 517 nm (*i.e.* violet colour), and when the DPPH solution is exposed to the CS-DTP/HA-CHO hydrogel it causes the decolourisation of the solution (*i.e.* yellow colour), indicating effective anti-oxidant activities. The results demonstrate that the CS-DTP/HA-CHO hydrogels have potential to reduce the overproduction of ROS, thereby relieving inflammatory responses and promoting wound healing.

3.7 *In vitro* biocompatibility and hydrogel ROS protection against H_2O_2 induced damage of cells

In vitro cell viability tests using the alamarBlue assay were performed with HaCaT cells to evaluate the biocompatibility of CS-DTP, CS-ADH, and HA-CHO polymers. LIVE/DEAD staining confirmed the viability of HaCaT cells and indicated low cytotoxicity in response to the materials. As shown in Fig. S4 and S5,† CS-DTP, CS-ADH, and HA-CHO maintained good cell viability when cocultured with polymer concentrations of 100, 500, and 1000 μg mL^{-1} for both 24 and 72 h.

To study the ROS protection effect of the CS-DTP/HA-CHO hydrogel, H_2O_2 (1 mM) was utilised to stimulate *in vitro* oxidative damage. Compared to the CS-ADH/HA-CHO control group, significantly improved cell survival was observed for the rADSCs and NHDFs encapsulated CS-DTP/HA-CHO hydrogels after 24 h co-culture (Fig. 5a). Live/dead images of hydrogel encapsulated rADSCs (Fig. 5b) show that the CS-DTP/HA-CHO hydrogels had a
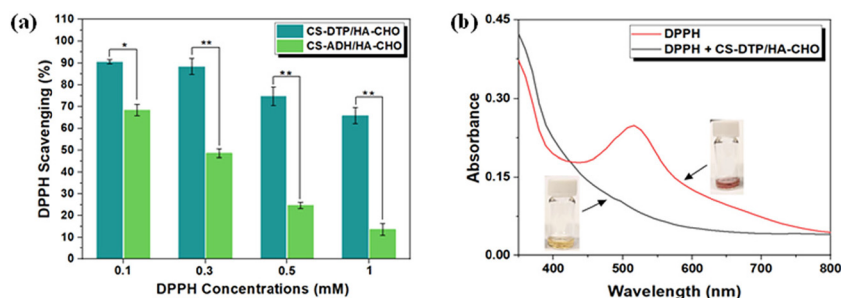

Fig. 4 Hydrogel antioxidative ability. (a) DPPH free radical scavenging ability of CS-DTP/HA-CHO and CS-ADH/HA-CHO hydrogels with a series of DPPH concentrations (0.1, 0.3, 0.5, and 1 mM); (b) UV-Vis spectra of DPPH (1 mM) after scavenging by CS-DTP/HA-CHO ($n = 3$, *$p < 0.05$, **$p < 0.01$).
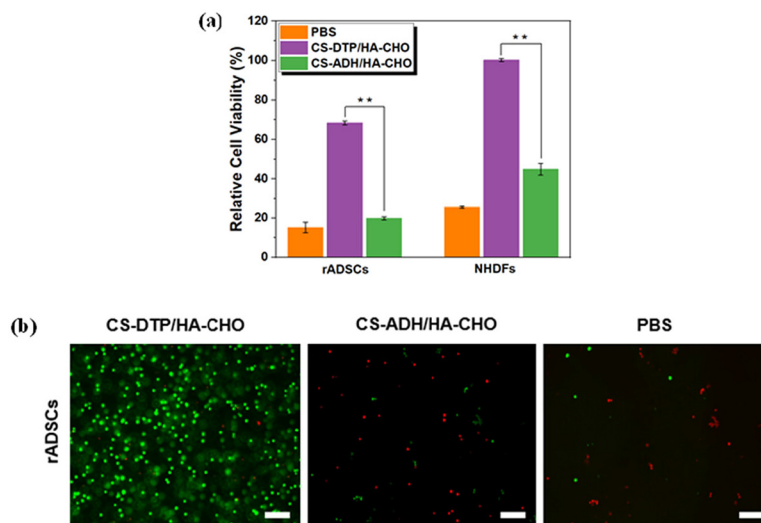
244 | *RSC Appl. Polym.*, 2025, **3**, 238–246

© 2025 The Author(s). Published by the Royal Society of Chemistry

Fig. 5 Effect of the CS-DTP/HA-CHO and CS-ADH/HA-CHO hydrogels on ROS protection of rADSCs and NHDFs in the presence of 1 mM H_2O_2. (a) Quantitative cell viability evaluation by alamarBlue assay; (b) representative live/dead staining images of ADSCs cell-seeded hydrogel at 24 h. Live cells are stained green (calcein AM) and dead cells are stained red (ethidium homodimer-1). Scale bar = 50 μm (**$p < 0.01$).

remarkably larger percentage of encapsulated live cells than the CS-ADH/HA-CHO control group and PBS. The results demonstrate that the viability of rADSCs and NHDFs are significantly influenced by ROS, and that the CS-DTP/HA-CHO hydrogel can effectively alleviate the ROS microenvironment and protect cells. This further highlights the excellent potential of the hydrogel system for use as antioxidative wound dressings and in other antioxidative biomedical applications. It is envisaged that the hydrogel formulation can be tailored to respond to different levels of ROS present in the wound environment, offering a degree of customisation that is currently lacking in current wound care products.

4. Conclusions

Large amounts of ROS can impel a wound to become a continuous inflammatory environment. Therefore, it is of great practical importance to design and develop dynamic materials with ROS scavenging properties for wound healing applications. In this study, a dynamic covalent polysaccharide-based hydrogel with ROS scavenging properties was designed with *in situ* formation and rapid gelation. Furthermore, the incorporation of the disulfide moiety into the hydrogel scaffold promoted responsive degradation behaviour and excellent ROS scavenging functions. Therefore, the CS-DTP/HA-CHO hydrogels offer valuable insights for designing dynamic hydrogels in biomedical applications, especially as antioxidative wound dressings for wound care treatments.

Author contributions

Conceptualization, M.J., S.A., and W.W.; methodology, M.J., and R.S.; software, W.W.; validation, M.J.; formal analysis, M.

J.; investigation, M.J. and R.S.; resources, W.W.; data curation, M.J.; writing – original draft preparation, M.J.; writing – review and editing, S.A., Y.L., C.M., J.L., Z.L., and W.W.; visualization, M.J. and S.A.; supervision, W.W.; project administration, W.W. All authors have read and agreed to the published version of the manuscript.

Data availability

The data supporting this article have been included as part of the ESI.†

Conflicts of interest

There are no conflicts to declare.

Acknowledgements

References

1 T. Velnar, T. Bailey and V. Smrkolj, *J. Int. Med. Res.*, 2009, **37**, 1528–1542.
2 P. Schilrreff and U. Alexiev, *Int. J. Mol. Sci.*, 2022, **23**, 4928.
3 C. Dunnill, T. Patton, J. Brennan, J. Barrett, M. Dryden, J. Cooke, D. Leaper and N. T. Georgopoulos, *Int. Wound J.*, 2017, **14**, 89–96.
4 L. Deng, C. Du, P. Song, T. Chen, S. Rui, D. G. Armstrong and W. Deng, *Oxid. Med. Cell. Longevity*, 2021, 8852749.

© 2025 The Author(s). Published by the Royal Society of Chemistry

RSC Appl. Polym., 2025, **3**, 238–246 | **245**

5 L. A. Pham-Huy, H. He and C. Pham-Huy, *Int. J. Biomed. Sci.*, 2008, **4**, 89–96.

6 N. I. Fadilah, S. J. Phang, N. Kamaruzaman and A. Salleh, *Antioxidants*, 2023, **12**, 787.

7 X. Li, X. Yang, Z. Wang, Y. Liu, J. Guo, Y. Zhu, J. Shao, J. Li, L. Wang and K. Wang, *Colloids Surf., B*, 2022, **209**, 112175.

8 A. Li, L. Li, B. Zhao, X. Li, W. Liang, M. Lang, B. Cheng and J. Li, *Int. J. Biol. Macromol.*, 2022, **194**, 914–923.

9 H. Zhong, J. Huang, M. Luo, Y. Fang, X. Zeng, J. Wu and J. Du, *Nanoresearch*, 2023, **16**, 599–612.

10 S. Cao, G. Xu, Q. Li, S. Zhang, Y. Yang and J. Chen, *Composites, Part B*, 2022, **234**, 109746.

11 Q. Xu, M. Venet, W. Wang, J. Creagh-Flynn, X. Wang, X. Li, Y. Gao, D. Zhou, M. Zeng, I. Lara-Sáez, S. A. H. Tai and W. Wang, *ACS Appl. Mater. Interfaces*, 2018, **10**, 39494–39504.

12 Z. He, Q. Xu, B. Newland, R. Foley, I. Lara-Sáez, J. F. Curtin and W. Wang, *J. Mater. Chem. B*, 2021, **9**, 6326–6346.

13 K. Y. Lee and D. J. Mooney, *Chem. Rev.*, 2001, **101**, 1869–1879.

14 S. Uman, A. Dhand and J. A. Burdick, *J. Appl. Polym. Sci.*, 2020, **137**, 1–20.

15 Y. Han and Y. Cao, *Gels*, 2022, **8**, 1–20.

16 D. Chen, G. Zhang, R. Li, M. Guan, X. Wang, T. Zou, Y. Zhang, C. Wang, C. Shu, H. Hong and L. J. Wan, *J. Am. Chem. Soc.*, 2018, **140**, 7373–7376.

17 C. De Gracia Lux, S. Joshi-Barr, T. Nguyen, E. Mahmoud, E. Schopf, N. Fomina and A. Almutairi, *J. Am. Chem. Soc.*, 2012, **134**, 15758–15764.

18 G. Wang, P. Huang, M. Qi, C. Li, W. Fan, Y. Zhou, R. Zhang, W. Huang and D. Yan, *ACS Omega*, 2019, **4**, 17600–17606.

19 S. Liu, S. Deng, T. Yan, X. Zhang, R. Tian, J. Xu, H. Sun, S. Yu and J. Liu, *Polymers*, 2021, **13**, 1–9.

20 H. T. Gebrie, K. D. Addisu, H. F. Darge, T. W. Mekonnen, D. T. Kottackal and H. C. Tsai, *J. Polym. Res.*, 2021, **28**, 1–13.

21 C. Yue, Y. Yang, C. Zhang, G. Alfranca, S. Cheng, L. Ma, Y. Liu, X. Zhi, J. Ni, W. Jiang, J. Song, J. M. de la Fuente and D. Cui, *Theranostics*, 2016, **6**, 2352–2366.

22 W. Song, J. You, Y. Zhang, Q. Yang, J. Jiao and H. Zhang, *Gels*, 2022, **8**, 361.

23 N. Ashwinkumar, S. Maya and R. Jayakumar, *RSC Adv.*, 2014, **4**, 49547–49555.

24 R. Yang, W. Xue, H. Liao, F. Wu, H. Guo, W. Zhang, P. Wang, X. Tan, H. Xu and B. Chi, *Int. J. Biol. Macromol.*, 2022, **223**, 950–960.

25 Q. Xu, M. Venet, W. Wang, J. Creagh-Flynn, X. Wang, X. Li, Y. Gao, D. Zhou, M. Zeng, I. Lara-Sáez, A. Sigen, H. Tai and W. Wang, *ACS Appl. Mater. Interfaces*, 2018, **10**, 39494–39504.

26 Y. Yang, H. Xu, M. Li, Z. Li, H. Zhang, B. Guo and J. Zhang, *ACS Appl. Mater. Interfaces*, 2022, **14**, 41726–41741.

27 J. Xu, Y. Liu and S. Hsu, *Molecules*, 2019, **24**, 3005.

28 S. Dawlee, A. Sugandhi, B. Balakrishnan, D. Labarre and A. Jayakrishnan, *Biomacromolecules*, 2005, **6**, 2040–2048.

29 M. Shafiq, Y. Chen, R. Hashim, C. He, X. Mo and X. Zhou, *Front. Bioeng. Biotechnol.*, 2021, **9**, 1–9.

30 S. Packiaraj, A. Pushpaveni, S. Govindarajan and J. M. Rawson, *CrystEngComm*, 2016, **18**, 7978–7993.

31 W. Shen, Q. Qiu, Y. Wang, M. Miao, B. Li, T. Zhang, A. Cao and Z. An, *Macromol. Rapid Commun.*, 2010, **31**, 1444–1448.

32 Z. Zhong, Z. Zhong, R. Xing, P. Li and G. L. Mo, *Int. J. Biol. Macromol.*, 2010, **47**, 93–97.